

Journal of Paleolimnology
Modeling the effect of convex upward deformation and horizontal sectioning on paleolimnological data
--Manuscript Draft--

Manuscript Number:		
Full Title:	Modeling the effect of convex upward deformation and horizontal sectioning on paleolimnological data	
Article Type:	Notes	
Keywords:	Coring; Deformation; 3D Model; Extrusion; Stratigraphy	
Corresponding Author:	Dewey Dunnington Acadia University Wolfville, NS CANADA	
Corresponding Author Secondary Information:		
Corresponding Author's Institution:	Acadia University	
Corresponding Author's Secondary Institution:		
First Author:	Dewey Dunnington	
First Author Secondary Information:		
Order of Authors:	Dewey Dunnington	
	Ian Spooner	
Order of Authors Secondary Information:		
Funding Information:	Natural Sciences and Engineering Research Council of Canada (CA) (130040)	Dr. Ian Spooner
Abstract:	We analyzed photos of convex upward deformation in split cores to obtain reasonable parameters with which to model the effect of convex upward deformation on paleolimnological data, and, using a 3-dimensional raster model, modeled the effect of this deformation on a hypothetical dataset. Results indicated that convex upward deformation integrates sample from an increasingly wider range of stratigraphic layers with increasing degree of deformation. After applying deformation, extruded concentration profiles were nearly identical despite varying the extrusion interval between 0.1 cm and 1 cm, suggesting there is a limit to the resolution attainable by horizontal sectioning if deformation occurred during sampling. Collectively our data suggest that determining the degree of deformation due to coring is essential prior to conducting high-resolution analysis of horizontally sectioned samples.	

[Click here to view linked References](#)1
2
3
4
5
6

Modeling the effect of convex upward deformation and horizontal sectioning on paleolimnological data

10
11 Dewey Dunnington (1), Ian Spooner (1)
12
13
14
15

(1) Department of Earth & Environmental Science, Acadia University, 12 University Ave. Wolfville, Nova Scotia, Canada B4P 2R5

16
17 Keywords: Coring, Deformation, 3D Model, Extrusion, Stratigraphy
18
19
20

Abstract

We analyzed photos of convex upward deformation in split cores to obtain reasonable parameters with which to model the effect of convex upward deformation on paleolimnological data, and, using a 3-dimensional raster model, modeled the effect of this deformation on a hypothetical dataset. Results indicated that convex upward deformation integrates sample from an increasingly wider range of stratigraphic layers with increasing degree of deformation. After applying deformation, extruded concentration profiles were nearly identical despite varying the extrusion interval between 0.1 cm and 1 cm, suggesting there is a limit to the resolution attainable by horizontal sectioning if deformation occurred during sampling. Collectively our data suggest that determining the degree of deformation due to coring is essential prior to conducting high-resolution analysis of horizontally sectioned samples.

52
53
54
55
56
57
58
59
60
61
62
63
64
65

1
2
3
4
5
6
7
8
9
10
11
12
13
14
15
16
17
18
19
20
21
22
23
24
25
26
27
28
29
30
31
32
33
34
35
36
37
38
39
40
41
42
43
44
45
46
47
48
49
50
51
52
53
54
55
56
57
58
59
60
61
62
63
64
65

Introduction

Deformation and compression of lake sediment during coring has long been known (Martin and Miller 1982; Wright 1993), and coring equipment design has attempted to minimize the conditions that promote deformation during coring (Martin and Miller 1982; Lane and Taffs 2002). Compression of sediment during coring is a widely accepted phenomenon (Glew et al. 2001), however convex upward deformation, while widely observed (Wright 1993; Rosenbaum et al. 2010), is infrequently discussed. Kegwin et al. (1998) noted a radial bias in paleomagnetic data from Ocean Drilling Program (ODP) piston cores and proposed a logarithmic function to model the deformation observed. Aubourg and Oufi (1999) noted a "conical fabric" develop due to "edge smearing" in soft sediments, also in relation to paleomagnetic data from ODP piston cores. Acton et al. (2002) revised the logarithmic function proposed by Kegwin et al. (1998), and created a model to correct paleomagnetic data for this bias. The logarithmic function proposed is a function of radius (r), core barrel radius (R), and degree of deformation (b).

$$(1) \quad Z(r) = -b \left(\ln\left(1 - \frac{r}{R}\right) + \frac{r}{R} \right)$$

Acton et al. (2002) estimate the b parameter of the equation is generally less than 0.2 but can range up to 0.4 in ODP piston cores (Fig. 1).

The idea that horizontal sectioning (extrusion) of deformed sediment is not ideal has been proposed (Rosenbaum et al. 2010), however the degree to which this deformation occurs and the effect that deformation has on paleolimnological data has not been investigated quantitatively. We suspect, given the large number of paleolimnological studies that use coring and extrusion to produce reproducible

1
2
3
4 results, that either deformation or its effect on the data is minimal. This paper is our
5 attempt to quantify and constrain the degree to which convex upward deformation
6 adds bias to horizontally sectioned paleolimnological data.
7
8
9
10
11
12
13

14 Methods

15

16 We used R statistical software (R Core Team 2013) to model, manipulate, and
17 visualize our data. Packages *dplyr* and *ggplot2* were used for manipulation and
18 visualization of data, respectively (Wickham et al. 2016; Wickham and Francois
19 202016).
21
22
23
24

25 Core photo analysis

26

27 To obtain reasonable parameters for b in our deformation function (Acton et al.
28 2002), we loaded 12 scale photos of deformed cores from 6 sources into image
29 analysis software and digitized deformed strata (Table 1). We performed a
30 regression on the digitized coordinates to estimate the degree of deformation (b) for
31 each layer.
32
33

34 Deformation model

35

36 We modeled horizontal sections with height H and diameter D as a 3-dimensional
37 raster grid with a cell size of 0.5 mm (Fig. 2). For each cell i , an original depth d_{0i} (i.e.
38 depth prior to convex upward deformation) was calculated with a reasonable range
39 of b parameters obtained from digitized strata. Density histograms were then
40 produced to estimate the contribution of each original depth d_0 to the slice. For each
41 slice, $d=0$ refers to the middle of the slice. We produced these models for $D=6.5$ cm,
42 as this represents the barrel width of our Glew (1989) gravity corer. Compression
43
44

1
2
3
4 was not modeled using this method, although modification of this model would
5
6 make including compression possible.
7
8
9

10 Effect on paleolimnological data
11

12 To model the concentration (mass fraction) we would obtain by sectioning and
13 homogenizing a sample with variable concentration and density, we need to
14 calculate total mass of the target substance divided by the mass of the slice. With a
15 3-dimensional raster grid using n cells, this value can be written as a sum of the
16 product of concentration (w), density (ρ), and volume (V) divided by the sum of the
17 product of V and ρ (2).
18
19
20
21
22
23
24
25
26
27

$$(2) \quad w_{avg} = \frac{\sum_{i=1}^n w_i \rho_i V_i}{\sum_{i=1}^n \rho_i V_i}$$

30 We can remove V_i from the summation in both the numerator and denominator
31 because the cell size is constant for each i , and write w and ρ as functions of d_{0i} .
32
33
34

$$(3) \quad w_{avg} = \frac{\sum_{i=1}^n w(d_{0i}) \rho(d_{0i})}{\sum_{i=1}^n \rho(d_{0i})}$$

35 Equation (3) in combination with our deformation model allows for modeling the
36 effect of sectioning, homogenization, and deformation given high-resolution un-
37 altered data. We used a generated dataset to test our deformation model inspired by
38
39 1 mm resolution XRF core scanner data (Guyard et al. 2007; Brunschön et al. 2010;
40 Kylander et al. 2011), and a linear dry density gradient from 0.1 to 0.5 g/cm³.
41
42 Generated data was transformed and smoothed random log normal data with a set
43
44 seed for replicability purposes.
45
46
47
48
49
50
51
52
53
54
55
56
57
58
59
60
61
62
63
64
65

1
2
3
4
Results
5
6

7
Core photo analysis
8

9 We digitized 49 deformed layers from 12 scale photos of split cores. The logarithmic
10 function was able to model most layers well (median r^2 of 0.84), but modeled some
11 layers poorly. The b coefficient ranged from 0.15 to 5.24, with a median of 0.78 (Fig.
12 3). We chose 0, 0.5, 1, and 2 as coefficients for our model to produce a reasonable
13 summary of the deformation that was observed (Fig. 4).
14
15

16 Deformation model
17
18

19 Slices of size 0.1 cm, 0.5 cm, and 1 cm were modeled with a core barrel diameter of
20 6.5 cm. When $d=0$, d_0 values ranged from 0 cm to -4 cm and were more negative
21 with increasing deformation (Fig. 5; Fig. 6). Slices represented a wider range of d_0
22 values with increasing deformation (Fig. 6; Fig. 7), and when deformation was >0.5,
23 slice sizes smaller than 1 cm did not result in decreasing the range of d_0 values.
24
25

26 Effect on paleolimnological data
27
28

29 As expected, increasing the thickness of the extrusion interval decreased the detail
30 that was visible in the data (Fig. 8). The original data include thin (<0.5 cm) layers of
31 high concentration (>60 units), only some of which were resolvable at extrusion
32 intervals greater than 1 mm. Peak values were lower with increasing extrusion
33 interval size, reflecting the inclusion of less concentrated material within the
34 interval. High values in the topmost sample are an artifact of the model; it is likely
35 that the behavior of deformation differs at the top of the core compared to
36 deformation below. Increasing the degree of deformation also decreased the ability
37 to resolve high concentration layers, decreased the peak concentration, and also
38
39

1
2
3
4 resulted in increasing the depth at which peak values were observed. When
5 deformation occurred, decreasing the extrusion interval size did not result in
6 increasing the effective resolution of the data. In particular, the extrusion interval of
7 0.1 cm and 0.5 cm produced nearly identical results when any deformation was
8 applied in our model.
9
10
11
12
13
14
15

16 17 18 **Conclusions** 19 20

21 The data indicated that even minimal deformation has an effect on
22 paleolimnological data. Many deformed core photos that were analyzed were of
23 cores collected by percussion coring, which can produce intense convex upward
24 deformation (Reasoner 1993), however some photos of split gravity cores also
25 contained observable deformation. Even when deformation was small, decreasing
26 the extrusion interval did not result in an appreciable difference in the
27 paleolimnological data (Fig. 8) or in decreasing the range of depths represented by
28 the slice (Fig. 7). Extrusion methods can produce sediment intervals of less than 0.1
29 cm (Cocquyt and Israël 2004), however our data suggest that reducing the extrusion
30 interval does not increase the effective resolution of the data if sediment has been
31 deformed by coring. Our data suggest that checking for deformation due to coring is
32 essential prior to conducting high-resolution analysis of horizontally sectioned
33 samples.
34
35
36
37
38
39
40
41
42
43
44
45
46
47
48
49
50
51
52
53
54
55
56
57
58
59
60
61
62
63
64
65

1
2
3
4
Acknowledgements
5
6
7
8
9
10
11
12
13
14
15

We acknowledge funding from the Natural Sciences and Engineering Research Council (NSERC) of Canada and the comments on this manuscript from the Department of Earth & Environmental Science at Acadia University.

16
Tables
17
18
19
20
21

Table 1 Sources of core photos that contained digitized layers used in this study.

Photo ID	Layers Digitized	Reference
cheak1	8	Menounos and Clague (2008)
cheak2	8	Menounos and Clague (2008)
crevice_lake	12	Rosenbaum et al. (2010)
ds_unpubl1	1	Dunnington and Spooner (unpublished data)
ds_unpubl2	2	Dunnington and Spooner (unpublished data)
ds_unpubl3	1	Dunnington and Spooner (unpublished data)
ds_unpubl4	1	Dunnington and Spooner (unpublished data)
longlake_pc1	1	White (2012)
suzielake_1	4	Spooner et al. (1997)
suzielake_2	9	Spooner et al. (1997)
whistler_gc4	1	Dunnington (2015)
whistler_gc8	1	Dunnington (2015)

44
Figures
45
46
47
48
49
50
51

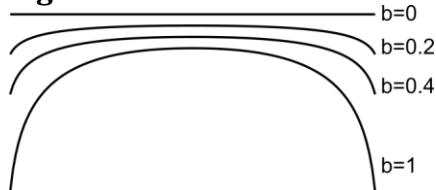


Fig. 1 Ideal patterns of deformation according to the logarithmic deformation function (Acton et al. 2002).

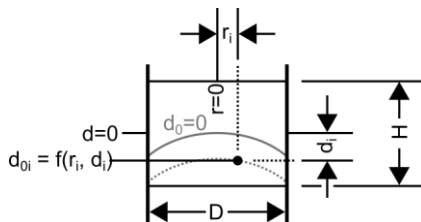


Fig. 2 Schematic of variables used in the deformation model. Models were produced for sections of diameter D and thickness H. Each point i in the section had a coordinate d_i and r_i , which were used to calculate the depth prior to convex upward deformation (d_{0i})

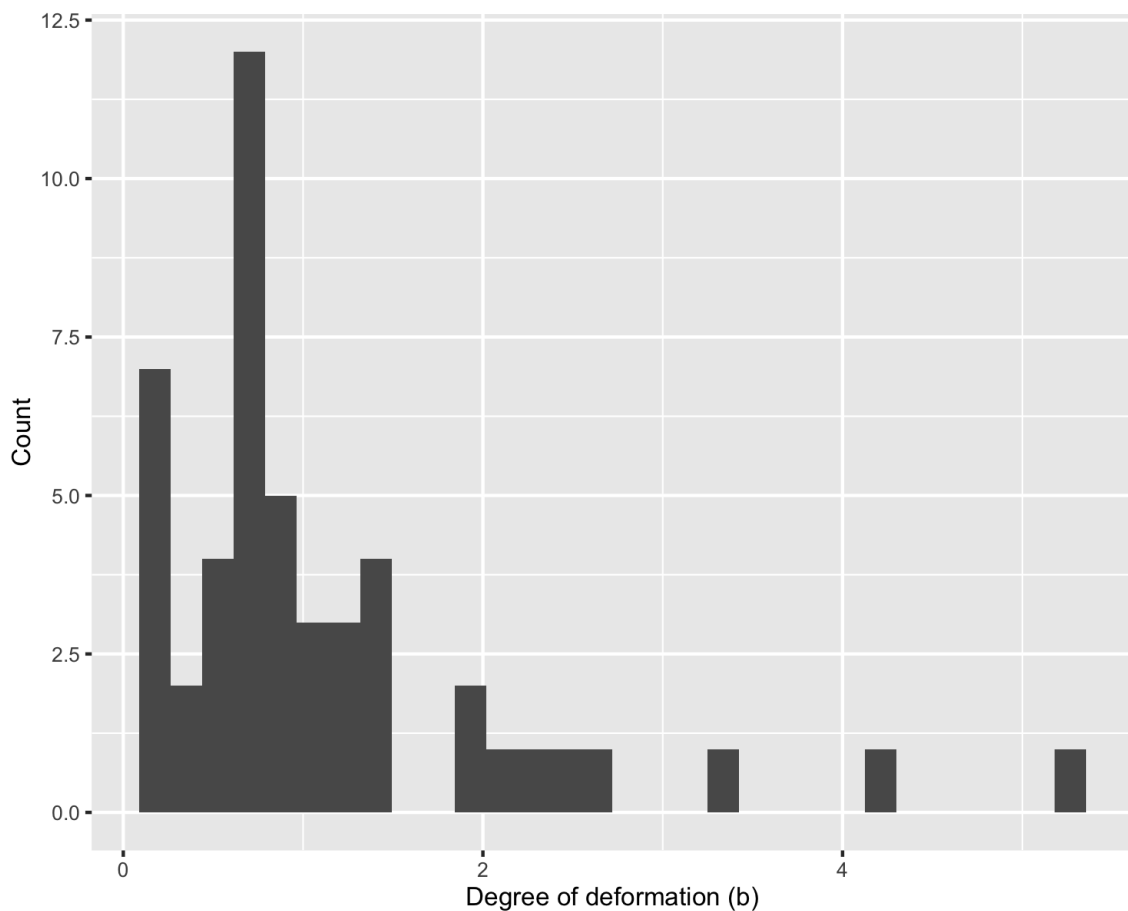
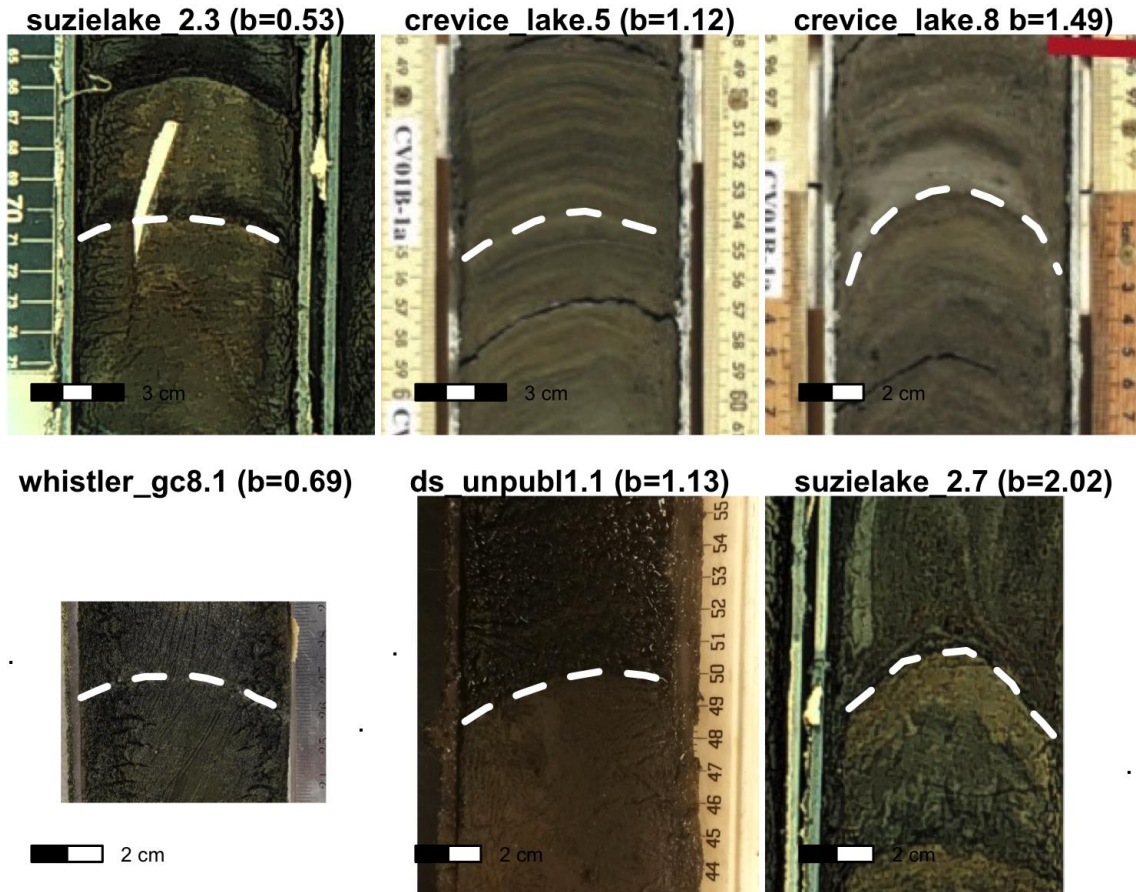


Fig. 3 Histogram of degrees of deformation (b) from digitized layers. Higher degrees of deformation corresponded to strata that were more deformed; lower degrees of deformation corresponded to strata that were less deformed.



37
 38
 39
 40
 41
 42
 43
 44
 45
 46
 47
 48
 49
 50
 51
 52
 53
 54
 55
 56
 57
 58
 59
 60
 61
 62
 63
 64
 65

Fig. 4 Representative layers for selected degrees of deformation.

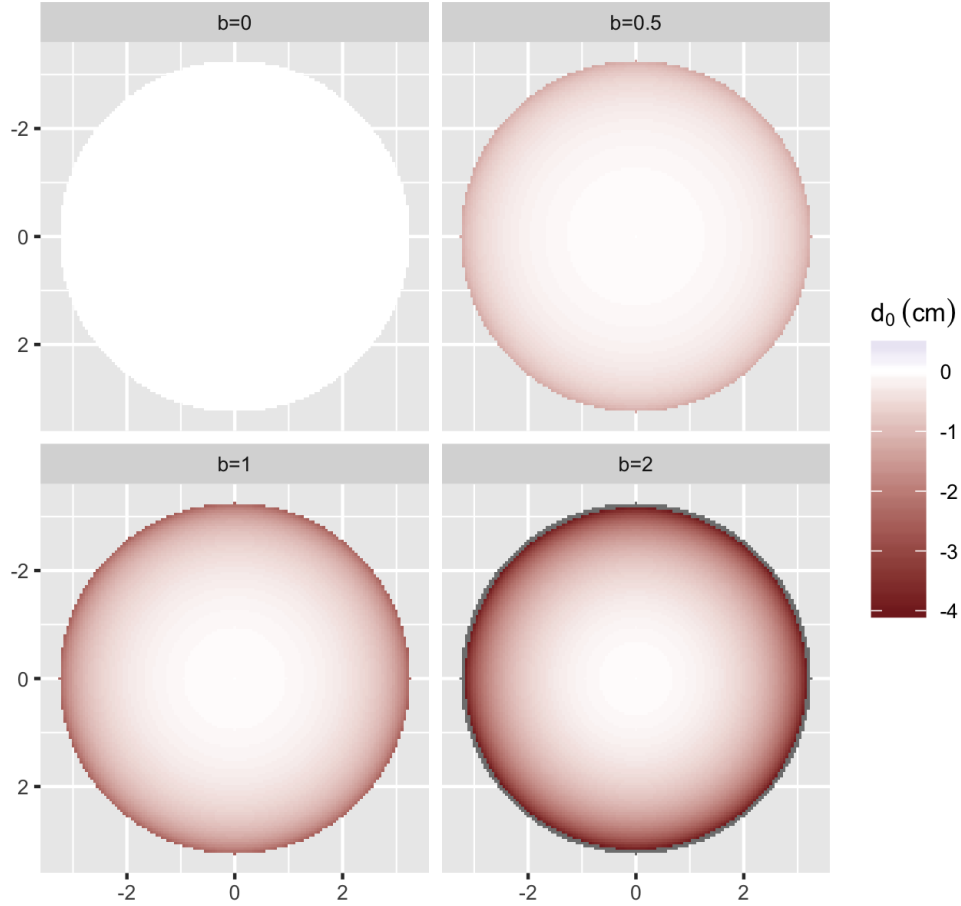


Fig. 5 Distribution of d_0 for $d=0$ by degree of deformation. Value $b=0$ indicates no deformation; $b=2$ indicates maximum deformation in the model. Coordinates are in centimeters.

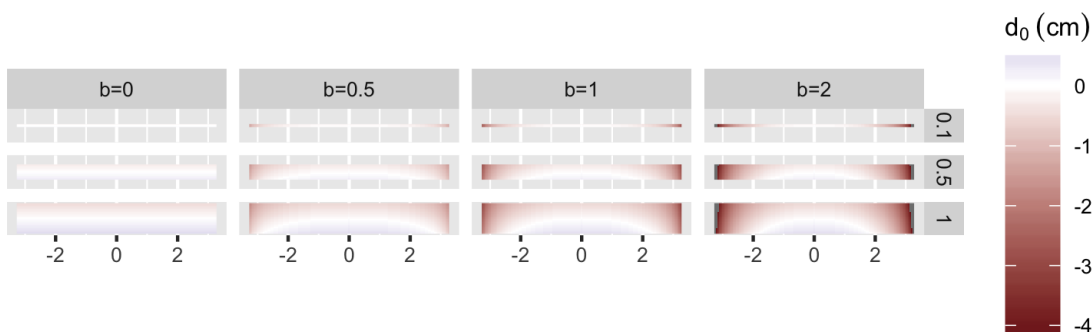


Fig. 6 Distribution of d_0 of a vertically sliced section for multiple degrees of deformation and slice sizes. Coordinates are in centimeters. Slice thickness is in centimetres and is indicated at right.

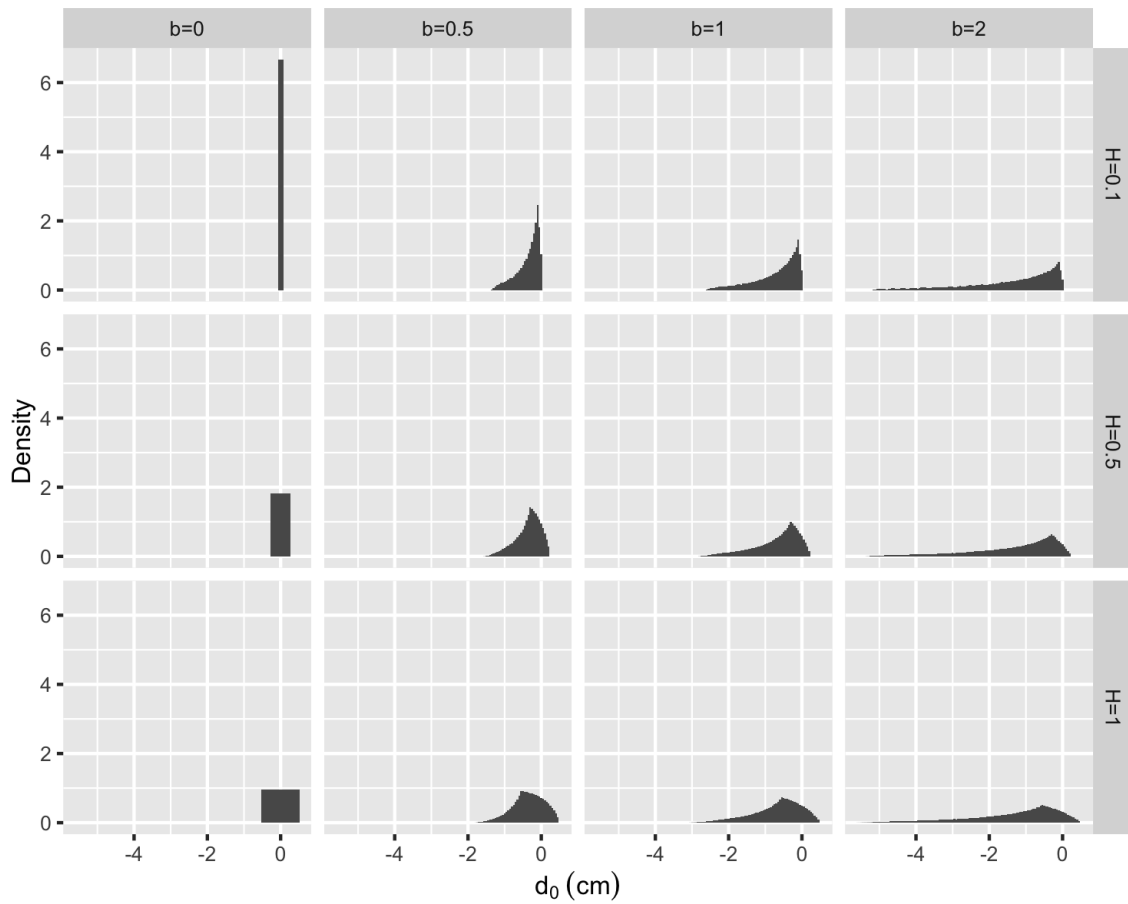


Fig. 7 Distribution of d_0 values modeled for multiple deformation coefficients and slice sizes. Wide distributions indicate that a wide range of original depths (d_0) contributed to that slice. Negative d_0 values in the distribution indicate the inclusion of strata from above the center depth of the slice.

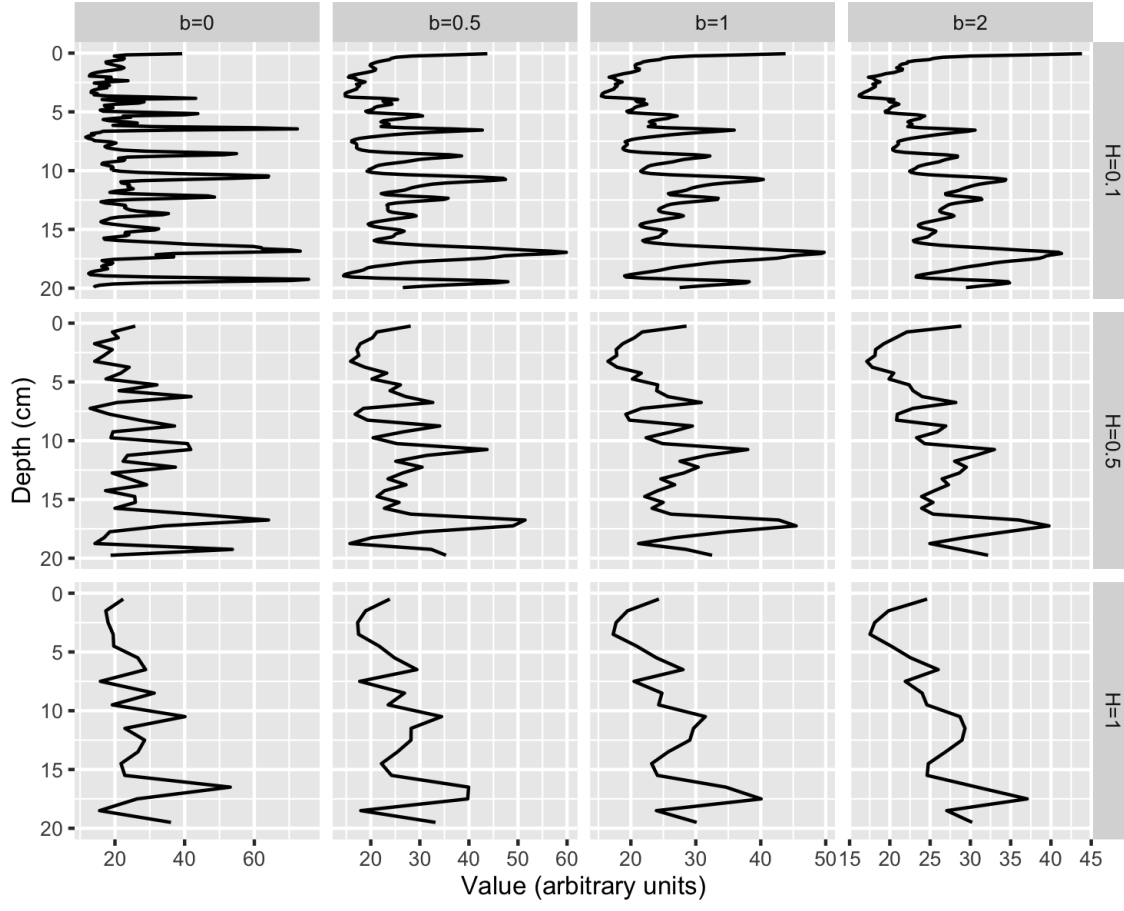


Fig. 8 Extrusion and deformation modeled for artificial 0.5 mm resolution concentration data. Original data is top left. Degree of deformation increases to the right; slice thickness increases toward the bottom.

1
2
3
4 **References**
5
6
7
8
9
10
11
12
13
14
15
16
17
18
19
20
21
22
23
24
25
26
27
28
29
30
31
32
33
34
35
36
37
38
39
40
41
42
43
44
45
46
47
48
49
50
51
52
53
54
55
56
57
58
59
60
61
62
63
64
65

- Acton GD, Okada M, Clement BM et al (2002) Paleomagnetic overprints in ocean sediment cores and their relationship to shear deformation caused by piston coring. *J Geophys Res* 107:EPM 3–1. doi: 10.1029/2001JB000518
- Aubourg C, Oufi O (1999) Coring-induced magnetic fabric in piston cores from the Western Mediterranean. In: *Proceedings of the Ocean Drilling Program: Scientific Results*. The Ocean Drilling Program, p 129
- Brunschön C, Haberzettl T, Behling H (2010) High-resolution studies on vegetation succession, hydrological variations, anthropogenic impact and genesis of a subrecent lake in Southern Ecuador. *Vegetation History and Archaeobotany* 19:191–206. doi: 10.1007/s00334-010-0236-4
- Cocquyt C, Israël Y (2004) A microtome for sectioning lake sediment cores at a very high resolution. *Journal of Paleolimnology* 32:301–304. doi: 10.1023/B:JOPL.0000042995.59566.85
- Dunnington DW (2015) A 500-year applied paleolimnological assessment of environmental change at Alta Lake, Whistler, British Columbia, Canada. M.Sc. Thesis, Acadia University
- Glew JR (1989) A new trigger mechanism for sediment samplers. *Journal of Paleolimnology* 2:241–243. doi: 10.1007/BF00195474
- Glew JR, Smol JP, Last WM (2001) Sediment core collection and extrusion. In: Last WM, Smol JP (eds) *Tracking environmental change using lake sediments*. Kluwer Academic Publishers, The Netherlands, pp 73–105

- Guyard H, Chapron E, St-Onge G et al (2007) High-altitude varve records of abrupt environmental changes and mining activity over the last 4000 years in the Western French Alps (Lake Bramant, grandes rousses massif). *Quaternary Science Reviews* 26:2644–2660. doi: 10.1016/j.quascirev.2007.07.007
- Kegwin L, Rio D, Acton GD (1998) Intermediate depth Blake outer ridge, sites 1056, 1057, 1058, and 1059. *Proceedings of the Ocean Drilling Program Initial Reports* 172:77–156. doi: doi:10.2973/odp.proc.ir.172.104.1998
- Kylander ME, Ampel L, Wohlfarth B, Veres D (2011) High-resolution X-ray Fluorescence core scanning analysis of Les Echets (France) sedimentary sequence: New insights from chemical proxies. *Journal of Quaternary Science* 26:109–117. doi: 10.1002/jqs.1438
- Lane CM, Taffs KH (2002) The LOG corer – a new device for obtaining short cores in soft lacustrine sediments. *Journal of Paleolimnology* 27:145–150. doi: 10.1023/A:1013547028068
- Martin EA, Miller RJ (1982) A simple, diver-operated coring device for collecting undisturbed shallow cores.
- Menounos B, Clague JJ (2008) Reconstructing hydro-climatic events and glacier fluctuations over the past millennium from annually laminated sediments of Cheakamus Lake, Southern Coast Mountains, British Columbia, Canada. *Quaternary Science Reviews* 27:701–713. doi: 10.1016/j.quascirev.2008.01.007

1
2
3
4 Menounos B, Clague JJ, Gilbert R, Slaymaker O (2005) Environmental reconstruction
5
6 from a varve network in the Southern Coast Mountains, British Columbia,
7
8 Canada. *Holocene* 15:1163–1171. doi: 10.1191/0959683605hl888rp
9
10

11 R Core Team (2013) R: A language and environment for statistical computing. R
12
13 Foundation for Statistical Computing, Vienna, Austria
14
15

16 Reasoner MA (1993) Equipment and procedure improvements for a lightweight,
17
18 inexpensive, percussion core sampling system. *J Paleolimnol* 8:273–281. doi:
19
20 10.1007/BF00177859
21
22

23 Rosenbaum JG, Skipp G, Honke J, Chapman C (2010) A composite depth scale for
24 sediments from Crevice Lake, Montana. United States Geological Survey,
25
26 Reston, Virginia
27
28

29 Spooner IS, Hills LV, Osborn GD (1997) Reconstruction of holocene changes in
30 alpine vegetation and climate, Susie Lake, British Columbia, Canada. *Arctic and*
31
32 *Alpine Research* 29:156–163. doi: 10.2307/1552042
33
34

35 White HE (2012) Paleolimnological records of post-glacial lake and wetland
36 evolution from the isthmus of chignecto region, eastern canada. M.Sc. Thesis,
37
38 Acadia University
39
40

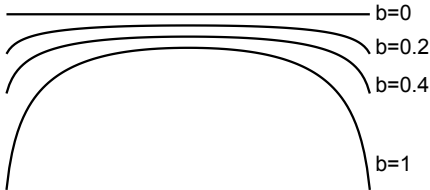
41 Wickham H, Chang W, RStudio (2016) Ggplot2: An implementation of the grammar
42
43 of graphics.
44
45

46 Wickham H, Francois R (2016) Dplyr: A grammar of data manipulation.
47
48

49 Wright HE (1993) Core compression. *Limnol Oceanogr* 38:699–701. doi:
50
51 10.4319/lo.1993.38.3.0699
52
53
54
55
56
57
58
59
60
61
62
63
64
65

Figure 1

Click here to
download



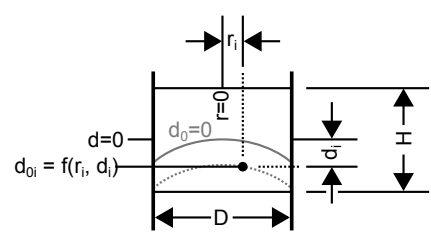
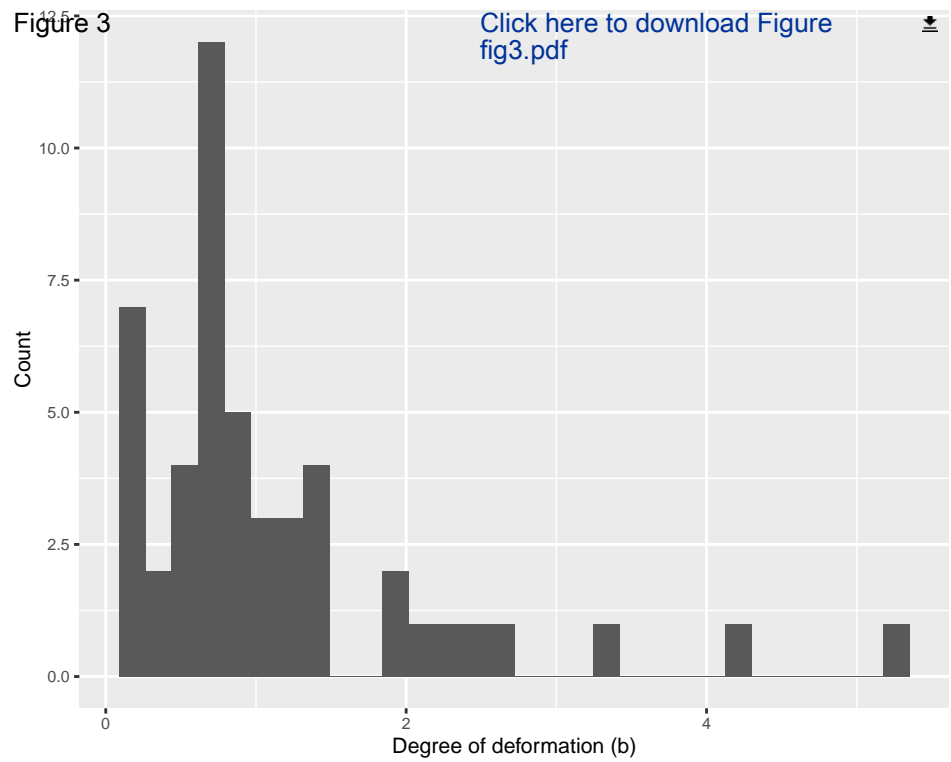


Figure 3

Click here to download Figure
fig3.pdf



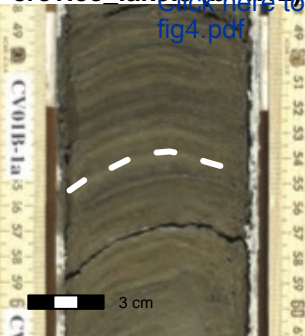
suzielake 2.3 (b=0.53)

Figure 4

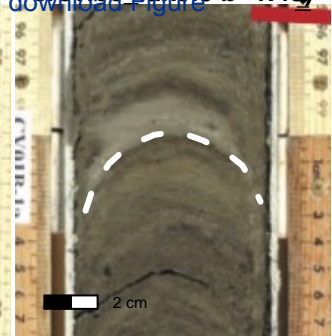


crevice_lake_5 (b=1.12)

Click here to download Figure fig4.pdf



crevice_lake_8 b=1.49



whistler_gc8.1 (b=0.69)

Figure 4



ds_unpubl1.1 (b=1.13)

Figure 4

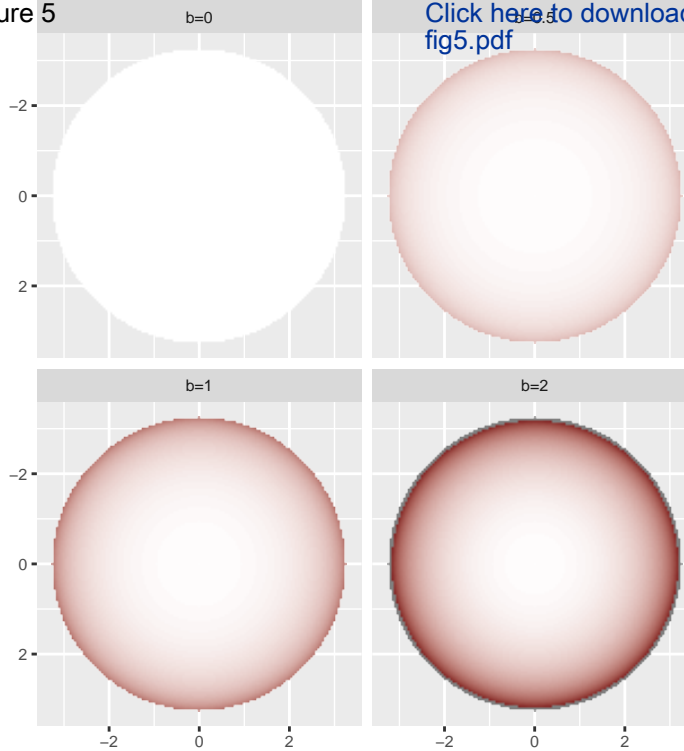


suzielake 2.7 (b=2.02)

Figure 4



Figure 5



[Click here to download Figure fig5.pdf](#)



Figure 6

[Click here to download Figure fig6.pdf](#)

d_0 (cm)

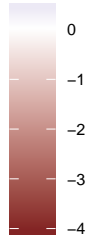
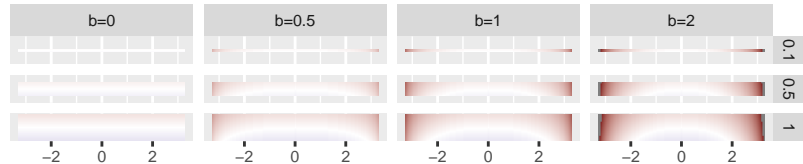
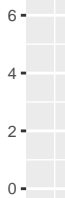


Figure 7 $b=0$ $b=0.5$

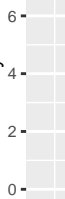
Click here to download Figure
fig7.pdf



Density

 -4 -2 0 d_0 (cm)

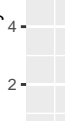
Density

 -4 -2 0 d_0 (cm)

Density

 -4 -2 0 d_0 (cm)

Density

 -4 -2 0 d_0 (cm)

Density

 -4 -2 0 d_0 (cm)

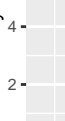
Density

 -4 -2 0 d_0 (cm)

Density

 -4 -2 0 d_0 (cm)

Density

 -4 -2 0 d_0 (cm)

Density

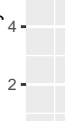
 -4 -2 0 d_0 (cm)

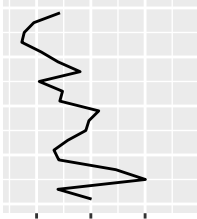
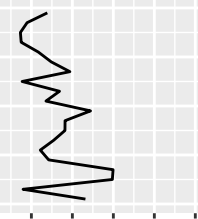
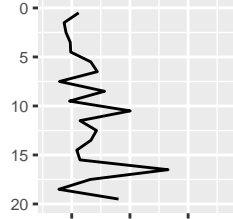
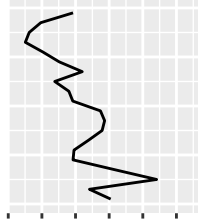
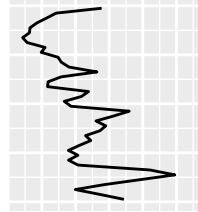
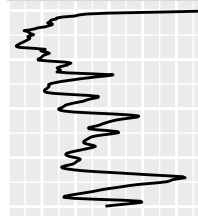
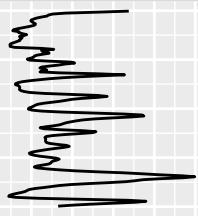
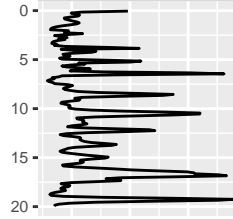
Figure 8

 $b=0$ $b=0.5$

Click here to download Figure
fig8.pdf

 $H=0.1$ $H=0.5$ $H=1$

Depth (cm)



Value (arbitrary units)

Table 1 Sources of core photos that contained digitized layers used in this study.

Photo ID	Layers Digitized	Reference
cheak1	8	Menounos and Clague (2008)
cheak2	8	Menounos and Clague (2008)
crevice_lake	12	Rosenbaum et al. (2010)
ds_unpubl1	1	Dunnington and Spooner (unpublished data)
ds_unpubl2	2	Dunnington and Spooner (unpublished data)
ds_unpubl3	1	Dunnington and Spooner (unpublished data)
ds_unpubl4	1	Dunnington and Spooner (unpublished data)
longlake_pc1	1	White (2012)
suzielake_1	4	Spooner et al. (1997)
suzielake_2	9	Spooner et al. (1997)
whistler_gc4	1	Dunnington (2015)
whistler_gc8	1	Dunnington (2015)